Biochemical Pharmacology 171 (2020) 113713

Contents lists available at ScienceDirect

Biochemical Pharmacology

journal homepage: www.elsevier.com/locate/biochempharm

Orabase-formulated gentian violet effectively improved oral potentially malignant disorder *in vitro* and *in vivo*

Yen Yun Wang[a,b], Ling Yi Xiao[b,c], Pao Chu Wu[d], Yuk Kwan Chen[a,b,e,f], Steven Lo[g], Stephen Chu Sung Hu[h,i], Yi Hua Chen[b,c], Charles Chien Chih Chiu[j], Shyng Shiou F. Yuan[b,c,k,l,m,*]

[a] School of Dentistry, College of Dental Medicine, Kaohsiung Medical University, Kaohsiung, Taiwan
[b] Center for Cancer Research, Kaohsiung Medical University, Kaohsiung, Taiwan
[c] Department of Medical Research, Kaohsiung Medical University Hospital, Kaohsiung Medical University, Kaohsiung, Taiwan
[d] School of Pharmacy, Kaohsiung Medical University, Kaohsiung, Taiwan
[e] Division of Oral Pathology & Maxillofacial Radiology, Kaohsiung Medical University Hospital, Kaohsiung,Taiwan
[f] Oral & Maxillofacial Imaging Center, College of Dental Medicine, Kaohsiung Medical University, Kaohsiung, Taiwan
[g] College of Medical, Veterinary and Life Sciences, University of Glasgow, Glasgow, UK
[h] Department of Dermatology, College of Medicine, Kaohsiung Medical University, Kaohsiung, Taiwan
[i] Department of Dermatology, Kaohsiung Medical University Hospital, Kaohsiung Medical University, Kaohsiung, Taiwan
[j] Chairman, Department of Biotechnology, Kaohsiung Medical University, Taiwan
[k] Translational Research Center, Kaohsiung Medical University Hospital, Kaohsiung Medical University, Kaohsiung, Taiwan
[l] Department of Obstetrics and Gynecology, Kaohsiung Medical University Hospital, Kaohsiung Medical University, Kaohsiung, Taiwan
[m] Graduate Institute of Medicine, College of Medicine, Kaohsiung Medical University, Kaohsiung, Taiwan

ARTICLE INFO

Keywords:
Oral potentially malignant disorder
Gentian violet
Orabase
Formulation

ABSTRACT

Oral cancer is a prevalent cancer in male worldwide. Oral potentially malignant disorders (OMPDs) are the oral mucosa lesions that have high malignant transformation rate to oral cancer. The mainstay for OMPDs treatment includes carbon dioxide (CO_2) laser and surgery, which may lead to the side effects of scarring and impaired function of oral cavity in the patients and reduced their willingness to receive curative therapy. Therefore, developing a non-invasive and function-preserving therapy is clinically important. Since development of a novel chemotherapeutic drug requires a lot of time and cost, we applied the high-throughput screening (HTS) approach to identify new bioactivities for FDA-approved drugs, known as drug repurposing. Through this drug repurposing approach, we discovered that gentian violet (GV), which is well known for its antibacterial, antifungal, antihelminthic, antitrypanosomal and antiviral activities, was able to induce significant cell death in DOK oral precancerous cells through ROS production. Moreover, decreased phosphorylation of p53(Ser15) and NFκB(Ser536) was required for GV-induced cell death. *In vivo*, 3% GV orabase effectively suppressed the progression of DMBA-induced oral precancerous lesions. In conclusion, this new formulation of GV through drug repurposing has the potential to be further developed as a therapeutic drug for OPMD clinically.

1. Introduction

Oral squamous cell carcinoma (OSCC) is the most common malignancy in the oral cavity and its early diagnosis is essential to reduce mortality and improve survival rate [1]. The five-year survival rate of OSCC is as low as 9% largely due to late diagnosis, often after metastasis has occurred [2]. The survival rate significantly improves to 60% ~85% if patients with OSCC are diagnosed and treated before lymph node infiltration [2,3]. Oral potentially malignant disorder (OPMD) includes various subtypes, including hyperplasia, leukoplakia, oral submucous fibrosis, erythroplakia and erythroleukoplakia, with the rate of developing OSCC ranging from 4% to 22% [4]. Moreover, it has been known that the risks of developing OSCC after 20 years of follow-up are 42.2% for leukoplakia and 95% for erythroleukoplakia [5]. Therefore, the diagnosis and management of this disease at the precancerous stage is likely to improve survival rates [6].

Surgery and radiotherapy are widely used for the treatment of early stage oral cancer (Stages I and II). However, potential side effects include scarring, difficulty in eating, dry mouth, flap failure, cosmetic disfigurement and functional loss in speech and swallowing [7]. Oral

* Corresponding author at: Center for Cancer Research, Kaohsiung Medical University, Kaohsiung, Taiwan.
E-mail addresses: wyy@kmu.edu.tw, yukkwa@kmu.edu.tw (Y.Y. Wang), pachwu@kmu.edu.tw (P.C. Wu), fyukkwa@kmu.edu.tw (Y.K. Chen), 940064@kmuh.org.tw (S.C.S. Hu), cchiu@kmu.edu.tw (C.C.C. Chiu), yanssf@kmu.edu.tw (S.S.F. Yuan).

https://doi.org/10.1016/j.bcp.2019.113713
Received 4 September 2019; Accepted 8 November 2019
Available online 14 November 2019
0006-2952/

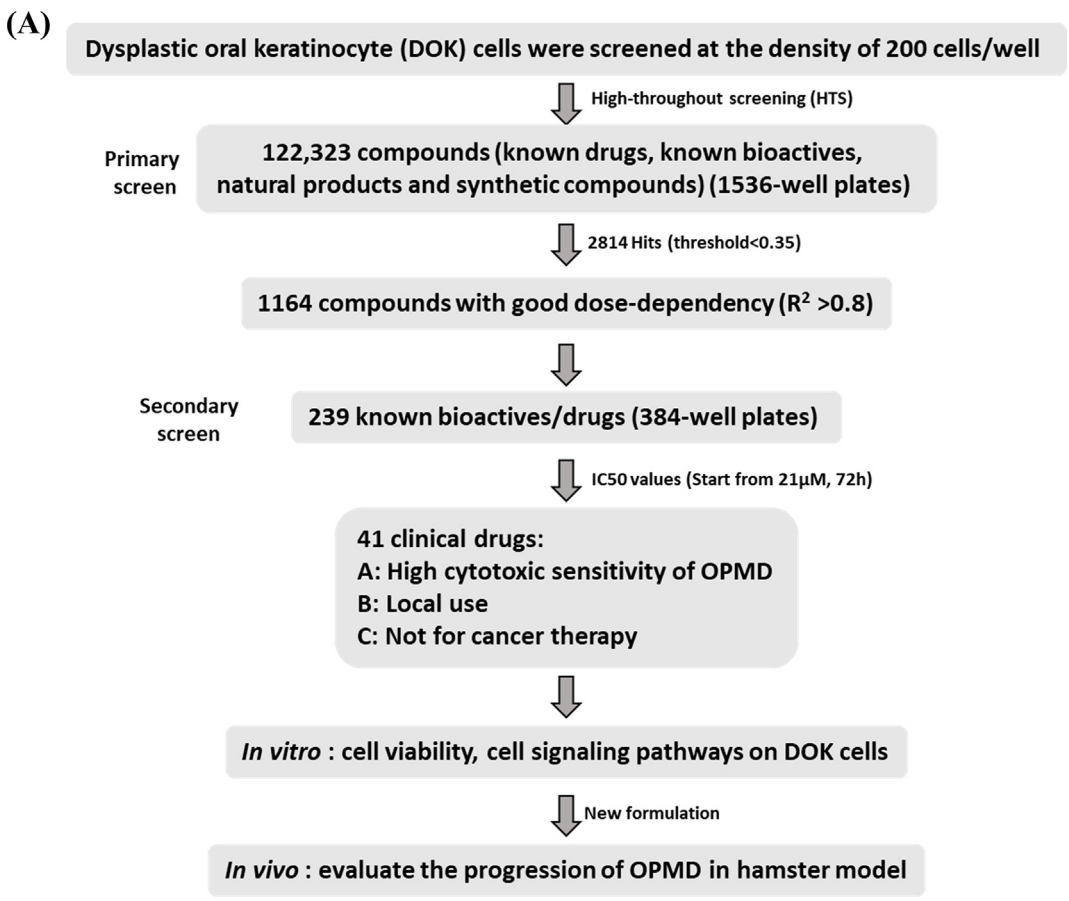

Compound Name	IC_{50} (μM)
Gentian Violet	0.02
Cisplatin	19.98

Fig. 1. HTS development and validation of anti-oral precancerous clinical drugs. (A) The flow chart for HTS assay. (B) In this activity histogram, a remaining activity less than 0.35 was used as the threshold to obtain the primary screening hits. (C) The IC_{50} of GV and cisplatin in DOK cells.

cancer is predominantly a local/regional disease. Although radiotherapy and surgery could specifically focus on the oral lesions, both treatment modalities are classified as invasive therapeutic approaches. Hence, developing a non-invasive and convenient orabase-formulated drug may improve the willingness of patients to receive treatment.

Gentian violet (GV) is a cationic triphenylmethane dye derived from aniline. In the field of therapeutic applications, GV has a long history of being used as an antibacterial, antifungal, anthelminthic, anti-trypanosomal and antiviral agent [8]. The therapeutic formulation of GV approved by the Food and Drug Administration (FDA) is the 1–2% GV solution [9]. Of note, GV has been reported to exhibit anticancer and anti-angiogenic activities in mice and humans [10,11]. In the oral cavity, GV has been approved for the treatment of oral candidiasis [12]. However, GV has not been previously investigated for treatment of oral precancerous lesions.

High-throughput screening (HTS) library could identify new bioactivities for previously approved drugs, a process known as drug repurposing [13]. In this report, we utilized a cell-based HTS assay to repurpose GV for the treatment of oral precancerous lesions. Herein, we demonstrated that GV showed significant cytotoxicity against oral precancerous cells, and orabase-formulated GV could improve oral precancerous lesions in the hamster model.

2. Material and methods

2.1. Cell culture

HOK human oral keratinocytes, DOK human oral precancerous cells

Table 1
The information and IC50 of the identified HTS hits.

	Compound Name	IC_{50} (μM)	SD of IC_{50} (μM)
1	JAK3 Inhibitor II	0.01	0.01
2	TX-1123	0.02	0.01
3	NSC 95397	0.07	0.02
4	Clomiphene citrate (Z,E)	0.27	0.09
5	Pyrvinium Pamoate	0.09	0.03
6	BAY 11-7082	0.27	0.06
7	Calmidazolium Chloride	0.13	0.02
8	Aklavine Hydrochloride	0.27	0.07
9	Tetramethylthiuram Monosulfide	0.12	0.02
10	Calcimycin A23187 Hemimagnesium Salt	0.07	0.01
11	Dronedarone	0.26	0.08
12	(S)-(+)-Niguldipine Hydrochloride	0.35	0.11
13	Totarol-19-Carboxylic Acid, Methyl Ester	0.25	0.04
14	A23187, Free Acid	0.02	0.01
15	Daunorubicin Hydrochloride	0.07	0.02
16	Teniposide	0.18	0.10
17	Ivermectin	0.34	0.11
18	GP 1a	0.58	0.23
19	Doxorubicin HCL	0.13	0.03
20	CDC25 Phosphatase Inhibitor III	0.26	0.06
21	Monensin sodium salt	0.06	0.01
22	Cantharidic Acid	0.16	0.02
23	Doxorubicin Hydrochloride	0.14	0.02
24	Calmidazolium chloride	0.26	0.08
25	Patulin	0.23	0.01
26	Wee1 Inhibitor II	0.19	0.03
27	Benzyldimethylcetylammonium Chloride	0.25	0.09
28	Phenylmercuric Acetate	0.03	0.01
29	EGFR Inhibitor III *TKS050*	0.03	0.01
30	Dequalinium Chloride	0.43	0.14
31	Daunorubicin	0.20	0.05
32	SIRT2 Inhibitor AGK2	0.17	0.03
33	TNF-alpha Inhibitor	0.31	0.04
34	Akt Inhibitor IX API-59CJ-OMe	0.15	0.05
35	Oxyphenbutazone	0.40	0.23
36	Cantharidin	0.20	0.04
37	Deoxysappanone B 7,4′-Dimethyl Ether	0.19	0.03
38	Fascaplysin Synthetic	0.33	0.06
39	Alexidine Hydrochloride	0.71	0.08
40	Cetrimonium Bromide	0.13	0.07
41	Auranofin	0.04	0.01
42	**Gentian Violet**	**0.02**	**0.01**
43	Tetrachloroisophthalonitrile	0.04	0.01
44	PD 153035 Hydrochloride	0.04	0.02
45	Cucurbitacin I Cucumis Sativus L.	0.02	0.01
46	NSC-632839	0.24	0.03
47	Anisomycin	0.23	0.09
48	Thonzonium bromide	0.21	0.04
49	Nsc 146109 Hydrochloride	0.43	0.09
50	PI3-Kalpha Inhibitor VIII	0.11	0.01
51	Pararosaniline Pamoate	0.23	0.05
52	Methylbenzethonium Chloride	0.93	0.34
53	Lapatinib	0.07	0.04
54	WHI-P97	0.07	0.03
55	Evodiamine Evodia rutaecarpa	0.29	0.09
56	TCMDC-125882	0.23	0.05
57	JAK3 Inhibitor IV	0.69	0.11
58	Mitomycin C	0.54	0.18
59	Ryuvidine	0.34	0.04
60	2-Phenylethynesulfonamide; Pifithrin-μ; NSC-303580	0.56	0.06
61	Homidium Bromide	1.11	0.23
62	Pimozide	0.57	0.09
63	Puromycin Dihydrochloride From Streptomyces Alboniger	0.11	0.04
64	Acetyl Isogambogic Acid	0.14	0.04
65	Lasalocid Sodium	0.73	0.20
66	5-Nitroso-8-quinolinol	0.6	0.06
67	Benzalkonium Chloride	0.56	0.23
68	Cerivastatin	0.09	0.04
69	Hexadecylpyridinium Chloride Monohydrate	0.06	0.03
70	Epirubicin Hydrochloride	0.03	0.00
71	Alsterpaullone 2-Cyanoethyl	0.30	0.03
72	CGP 71683 Hydrochloride	0.94	0.13
73	Demethylasterriquinone B1	1.43	0.06
74	Akt Inhibitor IV	0.37	0.14
75	SD-1029	1.19	0.25
76	Nogalamycin From Streptomyces Nogalater 395%	0.33	0.11
77	7BIO	1.08	0.22
78	Celastrol	0.17	0.03
79	Mitomycin C From Streptomyces Caespitosus	0.87	0.44
80	Doxorubicin	0.11	0.02
81	gamma-Secretase Inhibitor I	0.66	0.2
82	Triciribine	0.37	0.11
83	Amsacrine	2.16	0.76
84	eEF-2 Kinase Inhibitor NH125	0.30	0.15
85	Anthothecol	0.38	0.11
86	Mycophenolic Acid	0.31	0.15
87	Demethylasterriquinone B1	0.74	0.14
88	Oxibendazole	0.48	0.27
89	Rotenone	0.12	0.14
90	EGFR/ErbB-2 Inhibitor	0.48	0.14
91	Niclosamide	0.29	0.14
92	Gambogic Acid Amide	1.51	0.36
93	Anisomycin From Streptomyces Griseolus	0.21	0.05
94	Diethylstilbestrol	1.62	0.41
95	PI3-Kinase alpha Inhibitor IV	0.18	0.05
96	TPCA-1	0.45	0.23
97	Hinokitiol	0.72	0.30
98	LE 135	1.89	0.55
99	Pifithrin-mu	1.66	0.25
100	Cerivastatin	0.10	0.01
101	MG-115	0.35	0.06
102	KN-93	2.58	0.75
103	Scriptaid	1.22	0.62
104	Hexadecyltrimethylammonium Bromide	0.16	0.07
105	LY 83583	0.32	0.12
106	Histone Deacetylase Inhibitor III	1.50	0.55
107	Strophanthidin	0.11	0.04
108	Celastrol Celastrus Scandens	0.11	0.01
109	BPIQ-II	0.11	0.04
110	Tpl2 Kinase Inhibitor	1.18	0.19
111	Idarubicin	0.06	0.01
112	Ciclopirox Olamine	0.30	0.53
113	Albendazole	0.36	0.25
114	Doramectin	2.25	0.97
115	Bax Channel Blocker	0.43	0.14
116	JLK6; gamma-secretase inhibitor	2.91	0.39
117	5-Iodotubercidin	1.23	0.27
118	Dichlorophene	1.43	0.22
119	Proteasome Inhibitor IX AM114	1.69	0.42
120	Gambogic Acid	0.13	0.03
121	Withaferin A Withania somnifera	0.13	0.02
122	Mycophenolate	0.46	0.27
123	Diphenyleneiodonium Chloride	3.43	1.26
124	SR 33805 Oxalate	1.27	0.49
125	Staurosporine N-Benzoyl	0.82	0.23
126	beta-Secretase Inhibitor II	0.69	0.19
127	Cdk2/9 Inhibitor	0.07	0.01
128	Pararosaniline Hcl (Parafuchsin)	0.22	0.05
129	MG-132	0.31	0.16
130	Gitoxigenin Diacetate	0.32	0.06
131	Mycophenolic Acid	0.48	0.44
132	Narasin From Streptomyces Auriofaciens	2.72	1.46
133	Retinoic acid p-hydroxyanilide	0.33	0.2
134	R-7050	0.5	0.15
135	Lanatoside C	0.17	0.04
136	FCCP	0.26	0.02
137	RHC-80267	0.71	0.5
138	Aminopurvalanol A	2.23	0.92
139	MG 132	0.27	0.08
140	AG 879	1.75	0.45
141	RO-3306	2.33	1.32
142	gamma-Secretase Inhibitor XIV	0.19	0.11
143	Loteprednol etabonate	3.32	1.48
144	Verteporfin	1.58	1.52

(*continued on next page*)

Table 1 (*continued*)

	Compound Name	IC_{50} (μM)	SD of IC_{50} (μM)
145	Dihydrotanshinone I	2.39	0.89
146	Topotecan	0.20	0.07
147	Rebeccamycin From Saccharothrix Aerocolonigenes	1.31	0.57
148	Cdk4 Inhibitor	0.31	0.10
149	CGP 57380	2.22	1.45
150	Ivermectin	1.6	0.27
151	Pyrithione Zinc	0.11	0.03
152	HSV Replication Inhibitor BP5	1.81	0.54
153	Gitoxin	0.23	0.06
154	N'-(3-chlorophenyl)carbonohydrazonoyl dicyanide	0.69	0.20
155	NF-kappa B Activation Inhibitor III	3.97	5.93
156	Picropodophyllotoxin	1.41	1.40
157	Aurora Kinase Inhibitor III	2.14	0.51
158	Gsk-3 Inhibitor XIII	1.45	1.21
159	(Benzyloxycarbonyl)-Leu-Leu-phenylalaninal, ZLLF-CHO	0.73	0.32
160	Niclosamide	0.25	0.05
161	Deoxysappanone B 7,3′-Dimethyl Ether Acetate	2.83	1.18
162	Strophanthidinic Acid Lactone Acetate	0.43	0.23
163	Convallatoxin	0.15	0.05
164	Cdk1 Inhibitor	1.20	0.92
165	Harmine	0.76	0.37
166	Cdk4 Inhibitor	0.16	0.22
167	IMD0354	0.16	0.04
168	Fenbendazole	1.17	0.50
169	API-2	0.17	0.07
170	S-(Triphenylmethyl)-L-cysteine	0.71	0.33
171	Tyrphostin AG 879	3.1	0.63
172	Tunicamycin	0.19	0.07
173	AG 17	0.19	0.07
174	Hexachlorophene	0.96	0.32
175	Reversine	1.31	0.54
176	SB 225002	0.44	0.09
177	IMD-0354	0.56	0.02
178	PD-198306	0.28	0.06
179	Aminopurvalanol A	0.96	0.54
180	Flubendazol	0.68	0.53
181	CCT 018159	2.06	0.63
182	AS-252424	9.65	3.87
183	AS-605240	15.63	6.41
184	Dihydrorotenone	7.17	1.67
185	Indirubin Derivative E804	0.70	0.26
186	ZM 306416 hydrochloride	1.38	0.66
187	Proteasome Inhibitor I	1.72	0.4
188	Apoptosis Activator VI CD437/AHPN	2.33	1.22
189	Eg5 Inhibitor III Dimethylenastron	> 21	
190	IC261	> 21	
191	SNS-032	0.02	0.002
192	Lacidipine	0.58	0.22
193	RO-3306	0.91	0.31
194	Oxyphenbutazone	0.24	0.1
195	Lapatinib	0.16	0.05
196	Sertaconazole nitrate	0.72	0.20
197	Cetrorelix	2.66	0.84
198	Ebastine	0.43	0.09
199	3,5,4′-Tribromosalicylanilide	5.86	3.40
200	Podophyllotoxin Acetate	1.08	0.96
201	Thimerosal	0.24	0.05
202	Cryptotanshinone	4.09	0.87
203	Cedrelone	0.91	0.29
204	Pyrromycin	0.13	0.05
205	Sapindoside A	0.37	0.03
206	Mitoxanthrone Hydrochloride	0.81	0.32
207	Moxidectin	5.65	1.66
208	Amiodarone Hydrochloride	4.98	2.39
209	Derrubone	0.59	0.16
210	Puromycin Hydrochloride	1.37	0.50
211	Chloroxine	0.64	0.14
212	Evans Blue Tetrasodium Salt	1.38	0.69
213	Dequalinium Dichloride	0.63	0.17
214	5-Nonyloxytryptamine Oxalate	0.85	0.14
215	Bntx Maleate	3.85	0.74
216	SSH 79797 Dihydrochloride	0.25	0.13
217	Homoharringtonine	0.11	0.03
218	Gossypol	2.02	0.37
219	2-Methoxyestradiol	> 21	
220	Oxamflatin	0.53	0.18
221	Arcyriaflavin A Synthetic	0.04	0.03
222	BAY 11-7085	0.14	0.03
223	Histone Acetyltransferase Inhibitor II	0.87	0.29
224	Polyglutamine Aggregation Inhibitor III	1.53	0.51
225	IKK-2 Inhibitor VI	1.01	0.46
226	TGF-beta RI Inhibitor III *SB-505124*	1.25	0.4
227	OLDA	1.69	0.57
228	GTP-14564	0.72	0.06
229	AG 957 Adamantyl Ester	0.45	0.13
230	JAK3 Inhibitor V	0.31	0.06
231	LY 2183240	0.32	0.11
232	NNC 55-0396 dihydrochloride	0.59	0.20
233	PTPase CD45 Inhibitor	0.43	0.05
234	Afimoxifene; 4-Hydroxytamoxifen	1.13	0.29
235	Caffeic acid phenethyl ester	0.47	0.08
236	CGK 733	0.33	0.10
237	BMS 191011	0.31	0.08
238	PD 407824	0.60	0.24
239	10-DEBC hydrochloride	1.25	0.14
	Cisplatin	19.98	4.20

and SAS human oral cancer cells were used in this study (ATCC, USA). HOK cells were incubated with Oral Keratinocyte Medium (OKM) (ScienCell, USA) in pre-coated 2 μg/cm^2 poly-L-lysine (Merck, Germany). DOK and SAS cells were grown in Dulbecco's Modified Eagle Medium/Nutrient Mixture F-12 (DMEM/F12) (Gibco, USA) supplemented with 10% fetal bovine serum (BI, Israel), 100 U/mL penicillin, 100 μg/mL streptomycin, 1% L-glutamine and 1% non-essential amino acids (NEAA) (Gibco, USA). All cell lines were incubated at 37 ˚C with 5% CO_2.

2.2. High-throughput screening assay

The primary screening was performed in 1536-well plates at the Genomics Research Center of Academia Sinica in Taiwan. For HTS assay development, different culture media and freezing media were first tested to select the best choices for large-scale cell preparation. For assay development, various numbers of DOK cells (100~5000 cells/well) in various concentrations of FBS were dispensed into wells of a 1536-well plate. After 48 h or 72 h incubation, cell proliferation was measured using Cell TiterGlo (Promega). The CV% and Z' value of HTS were determined as 8~10% and 0.63, respectively. The primary hits of interest were selected for determining IC_{50} values in the secondary screening.

2.3. XTT assay

DOK cells were seeded at 5 × 10^3 cells/well in 96-well plates and allowed to attach overnight. After treatment with different experimental conditions for 24 h, cell viability was assessed by the XTT assay (Merck, USA) according to a previous study [14].

2.4. Cell cycle distribution

1.5 × 10^5 DOK cells were seeded in 6-well plates and allowed to attach overnight. After treatment with GV, NAC, PFT-α (Merck, USA) and/or BAY11-7085 (TaiClone, Taiwan) for 24 h, DOK cells were harvested and stained with PI staining solution (0.02 mg/mL PI, 0.2 g RNaseA and 0.05% Triton-X 100 in PBS) (Merck, USA) at room temperature for 10 min. The samples were analyzed by Beckman Flow

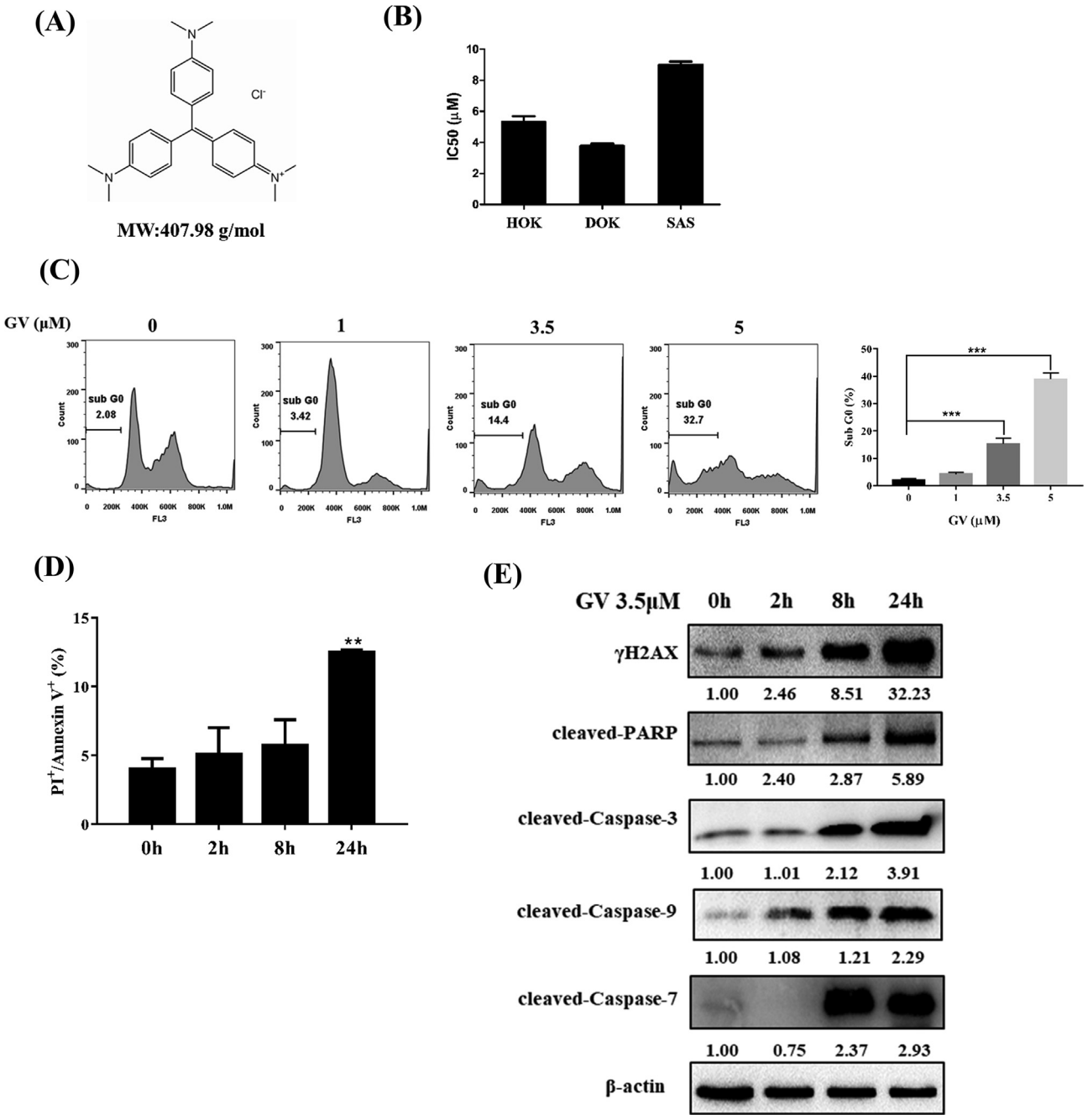

Fig. 2. Determination of the anti-oral precancerous activity of GV. (A) The chemical structure of GV. (B) HOK normal epithelial cells, DOK oral precancerous cells and SAS oral cancer cells were treated with various concentrations of GV for 24 h and then cell viability was assessed by the XTT assay. (C) DOK cells were treated with 1 μM, 3.5 μM or 5 μM GV for 24 h. Harvested cells were stained by PI and cell cycle was analyzed by flow cytometry. (D) DOK cells were treated with 3.5 μM GV for 2 h, 8 h and 24 h. Harvested cells were stained with PI/Annexin V and analyzed by flow cytometry. (E) The expression of apoptosis-related proteins in DOK cells treated with 3.5 μM GV for 2 h, 8 h and 24 h were analyzed by immunoblotting. The expression of β-actin was used as the internal control. Columns represent the mean of three experiments and error bars indicate SE. **p < 0.005; ***p < 0.0005.

Cytometer and the data were analyzed with Flow Jo software.

2.5. PI/Annexin V staining

1.5×10^5 DOK cells were seeded in 6-well plates and allowed to attach overnight. After treatment with GV, NAC, PFT-α and/or BAY11-7085 for 24 h, DOK cells were harvested and stained with Annexin V-FITC and PI (BD, USA) at room temperature for 20 min. The samples were analyzed by Beckman Flow Cytometer and the data were analyzed with Flow Jo software.

2.6. Western blotting

6×10^5 DOK cells were seeded in 6-cm plates and allowed to attach overnight. After treatment with GV, PFT-α or BAY11-7085 for 0.5 h, 2 h, 4 h or 24 h, DOK cells were harvested and lysed in RIPA buffer supplemented with proteinase inhibitor. The lysates were separated by SDS-PAGE, transferred to PVDF membrane (PALL, USA), and blotted with primary antibodies and secondary antibodies (Jackson, USA). Subsequently, the signal was analyzed by ECL (Perkin Elmer, USA) and ChemiDoc™ XRS+ System with Image Lab™ (BioRad, USA). Primary antibodies including anti-pp53(ser15) [15], anti-p53 [16], anti-γH2AX

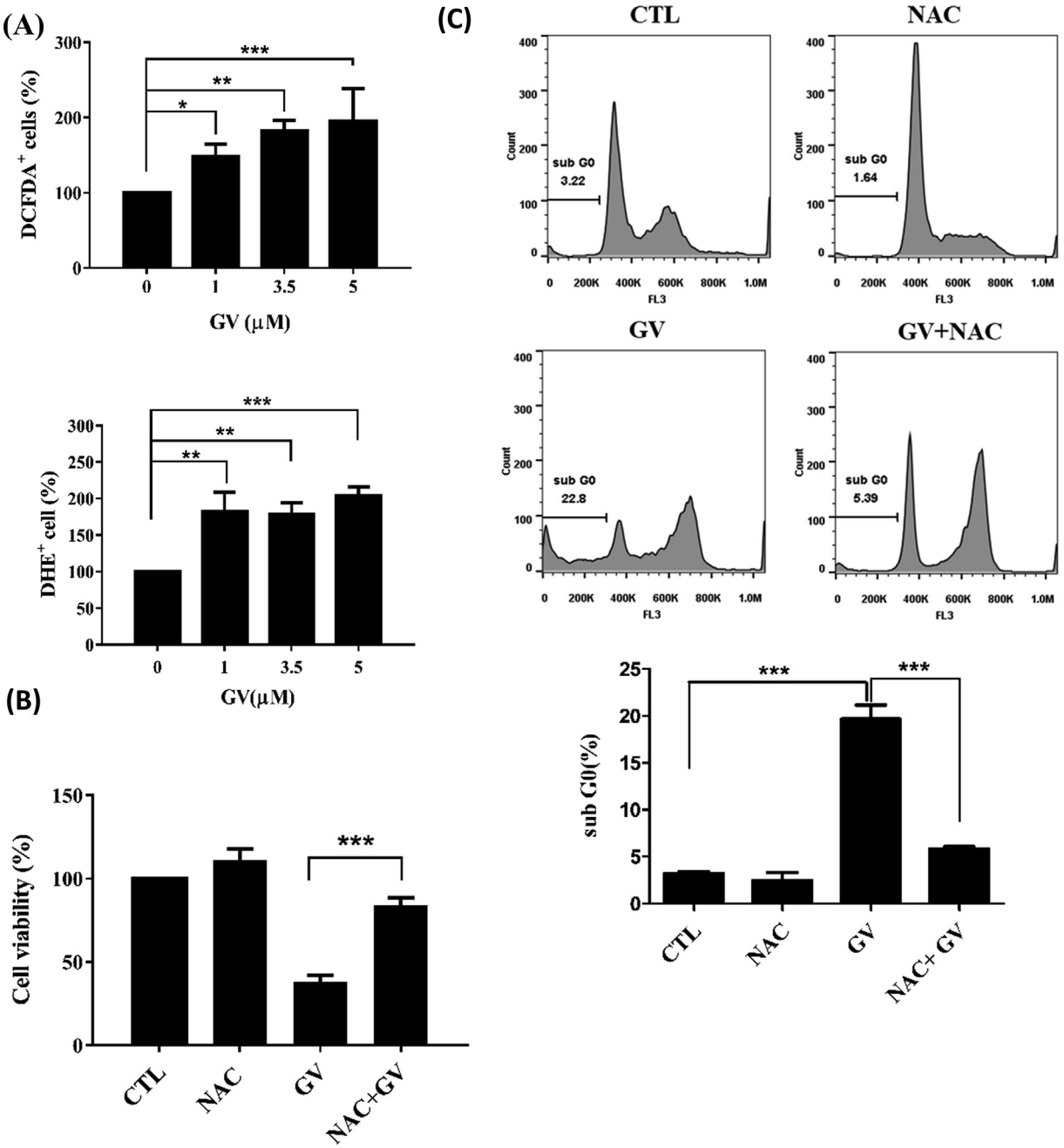

Fig. 3. ROS generation was involved in GV-induced cell death in oral precancerous cells. (A) DOK cells were treated with 1 μM, 3.5 μM or 5 μM GV for 1 h and ROS level was determined by DCFDA or DHE staining. Fluorescent intensity was determined by flow cytometry. (B) DOK cells were treated with 3.5 μM GV alone or together with 10 mM NAC for 24 h. The cell viability was assessed by the XTT assay. (C) DOK cells were treated with 3.5 μM GV alone or together with 10 mM NAC for 24 h. The cell cycle was assessed by PI staining and flow cytometry. Columns represent the mean of three experiments and error bars indicate SE. ***$p < 0.0005$.

[17], anti-Ki67, anti-Actin [18] and anti-GAPDH [19]were obtained from GeneTex (USA), while anti-NFκB [20], anti-cleaved caspase-3 [21], anti-cleaved caspase-9 [22], anti-cleaved caspase-7 [23], anti-cleaved PARP [24] antibody was obtained from Cell Signaling (USA). The antibody of anti-pNFκB(ser536) was obtained from Abcam (UK) [25]

2.7. Reactive oxidative stress (ROS) detection

DOK cells were seeded at 1.5×10^5 cells/well in 6-well plates and allowed to attach overnight. After treatment with 3.5 μM GV for 1 h, intracellular ROS content was measured using DCFDA and DHE fluorescent dyes (BD, USA). DOK cells were stained with 10 μM of DCFDA or DHE for 30 min in the dark. The mean fluorescence intensity was measured by Beckman Flow Cytometer and the data were analyzed with Flow Jo software.

2.8. Orabase formulation of gentian violet

Hydroxypropylmethylcellulose 4000 (HPMC4000) is used as a thickening agent, binder, film former, and hydrophilic matrix material for orabase formulation of gentian violet. HPMC4000 (5%), Ethanol (10%), GV (10%) and distilled water were used to prepare orabase formulation of GV. Accurately weighed quantity of GV was dissolved and mixed in distilled water for at least 12 h. Then, 5% HPMC4000 and 10% Ethanol were sequentially incorporated into the mixture. Orabase-

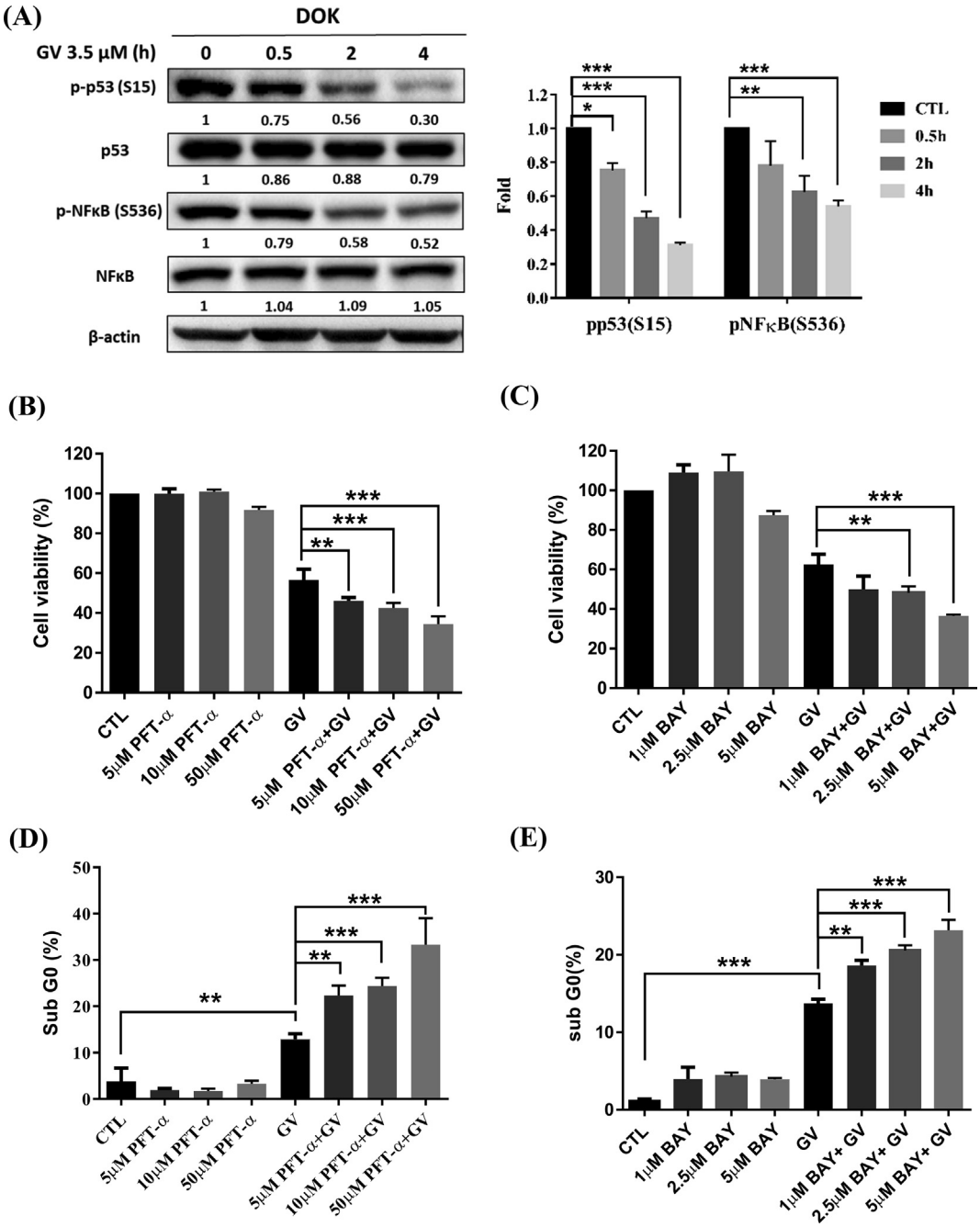

Fig. 4. The signaling pathways regulated by GV in oral precancerous cells. (A) The expression of p-p53(S15), p53, p-NFκB(S536) and NFκB in DOK cells treated with 3.5 μM GV for 0.5 h, 2 h and 4 h. β-actin was used as the internal control. (B) DOK cells were treated with 5 μM, 10 μM and 50 μM PFT-α and p-p53(S15) expression and cell viability were determined. (C) DOK cells were treated with 1 μM, 2.5 μM and 5 μM BAY11-7085 and analyzed for p-p53(S15) expression and cell viability. (D) DOK cells were treated with 5 μM, 10 μM and 50 μM PFT-α alone or in combination with 3.5 μM GV for 24 h, and cell cycle was analyzed by flow cytometry. (E) DOK cells were treated with 1 μM, 2.5 μM and 5 μM BAY11-7085 alone or in combination with 3.5 μM GV for 24 h. Cell cycle was analyzed by flow cytometry. Columns represent the mean of three experiments and error bars indicate SE. *p < 0.05; **p < 0.005; ***p < 0.0005.

formulated GV was stored in a closed brown bottle.

2.9. Animal model

The hamster buccal pouch mucosa is one of the most widely accepted experimental models of oral carcinogenesis [26] for the buccal pouch is easy to spread out and treated with drugs. The animal study was approved by the Institutional Animal Care and Use Committee of Kaohsiung Medical University and was conducted in accordance with the Animal Research: Reporting *in Vivo* Experiments (ARRIVE) guidelines. In this study, 7,12-dimethylbenz[a]anthracene (DMBA) (MERCK, USA) was applied on the buccal pouch of hamsters to induce oral precancerous lesions [27,28], followed by 3% GV treatment once a week with the time scheme illustrated in Fig. 5A. Sixteen outbred male Syrian golden hamsters (Mesocricatus auratus), weighing 80–100 g each at the start of the experiment, were randomly assigned into one of the following four groups. The untreated group (Group A, n = 2) consisted of hamsters without any treatment. The GV-treated group (Group B, n = 2) consisted of hamsters with 3% GV treatment only. For the experimental groups (Group C and D), the buccal pouch was painted 10 times with 0.5% DMBA (in mineral oil) three times per week for 9 weeks. The DMBA-treated group (Group C, n = 3) were only

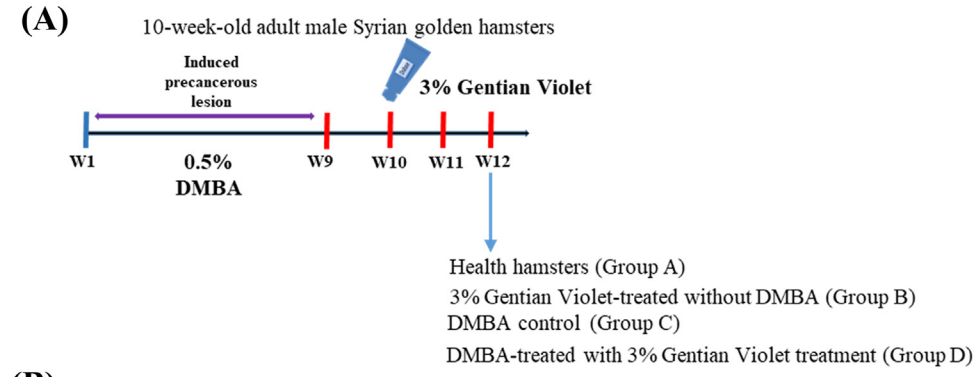

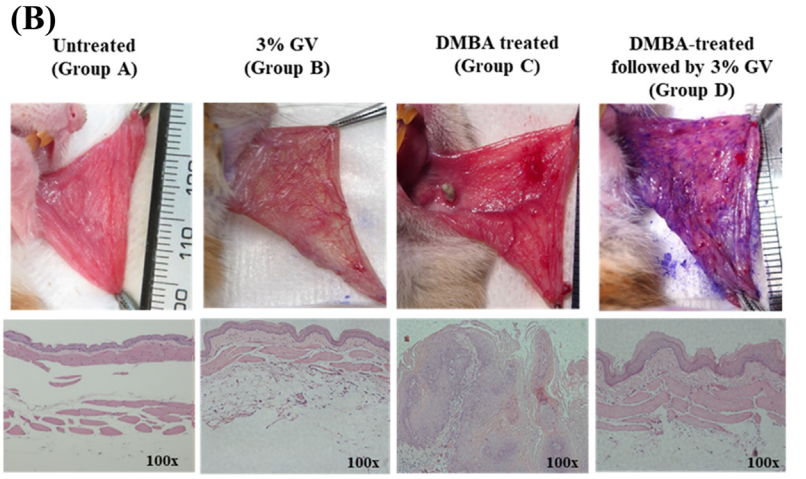

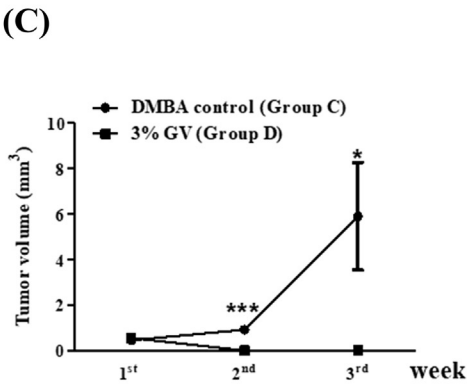

(D)

	Group B	Group C	Group D
AST/SGOT (U/L)	71.50±27.55	52.50±4.95	66.43±22.51
AST/SGPT (U/L)	73.50±12.5	63.33±15.82	53.83±6.37
BUN (mg/dL)	18.65±3.05	20.17±1.23	21.40±0.83
Creatinine (mg/dL)	0.29±0.02	0.26±0.03	0.27±0.01

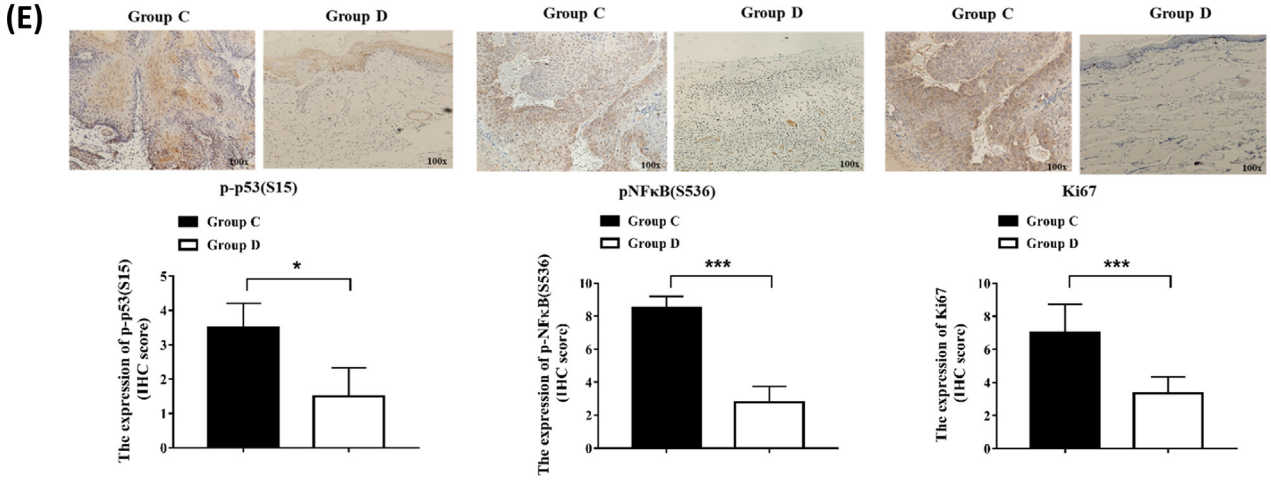

Fig. 5. GV suppressed the progression of oral precancerous lesions. (A) The flow chart for the experimental design. (B) Clinical images and H&E stains taken from four experimental groups: untreated group (Group A); GV-treated group (Group B), DMBA-treated group (Group C) and DMBA-treated group followed by 3% GV (Group D). (C) Average tumor volumes were measured and compared between Group C and Group D according to the formula "(width^2 × length)/2". (D) Blood biochemical profile of the hamsters was analyzed at the end of 12 weeks. The expression of (E) p-p53(S15), p-NFκB(S536) and Ki67 from Group C and Group D hamsters were analyzed by immunohistochemistry. Columns represent the mean of three experiments and error bars indicate SE. *p < 0.05 ***p < 0.0005.

treated with DMBA. Hamsters in Group D (n = 9) were treated with DMBA followed by 3% GV treatment once a week for three weeks. Hamsters were euthanized at the 12th week by injecting Zoletil® (VIRBAC, French) before CO_2 asphyxiation. Tumor size was measured once a week and tumor volume was calculated according to a standard formula: (width^2 × length)/2.

2.10. Immunohistochemistry and hematoxylin-eosin staining

Oral mucosa tissues from the buccal pouches of hamsters were excised and fixed in 10% neutral-buffered formalin solution for 24 h, followed by histological processing and paraffin embedding. Tissue sections were obtained and mounted on glass slides for further experiments. Immunohistochemical staining for p-p53(ser15), p-NFκB (ser536) and Ki67 were performed using the fully automated Bond-Max system and in accordance with the manufacturer's instructions (Leica Microsystems, Wetzlar, Germany). For quantification of p-p53(ser21), p-NFκB(ser536) and Ki67 staining, the percentage of positively stained tumor cells was graded according to the following categories: 0 (0–4%), 1 (5–24%), 2 (25–49%), 3 (50–74%) or 4 (75–100%) [29–32]. In addition, the global staining intensity was scored as 0 (negative), 1 (weak), 2 (moderate) or 3 (strong). The total immunostaining score was calculated as the percentage of positively stained cells multiplied by the global staining intensity. In addition, the tissues from buccal pouches of hamsters were stained with hematoxylin-eosin.

2.11. Statistical analysis

All observations were confirmed by at least three independent experiments. Data were expressed as mean ± standard error (SE). Differences between experimental groups were determined by one-way analysis of variance (ANOVA) with post hoc Tukey's test for multiple comparisons. Independent *t*-test was used for the comparison between two groups of data. P value < 0.05 was regarded to be statistically significant.

3. Results

3.1. HTS screening of clinical drugs with anti-oral precancer activity

The primary HTS assay was adapted into a 1536-well plate format through optimization of several parameters, including the incubation time (72 h), number of oral precancerous cells (2000) and concentration of FBS (2%) for screening of 122,323 compounds (Fig. 1A). According to the activity profiles of compounds, a total of 2814 hits in which the activity was smaller than 0.35 were selected for further confirmation and IC_{50} determination (Fig. 1B). The IC_{50} values of 1164 compounds from 2814 hits showed good dose-dependency (R^2 > 0.8) (data not shown and will be provided if requested). Next, a total of 239 known bioactive compounds/drugs from primary screening were selected to determine their IC_{50} values in 384-well plates (Table 1). From the secondary screening results, 41 clinical drugs fulfill three criteria, including high cytotoxicity against oral precancerous cells, able to be locally used and previous indications not including cancer therapy. After selection by HTS assay, we used the potential compounds for *in vitro* experiments and new formulations of the potential compounds for *in vivo* experiments. Since cisplatin is clinically used for the treatment of oral cancer, the IC_{50} of cisplatin in DOK oral precancerous cells was used as a positive control to verify the cytotoxic potential of the screened compounds. According to the result from screening, we found that the IC_{50} of GV was 0.02 μM, which was lower than the IC_{50} of cisplatin (20 μM) (Fig. 1C).

3.2. Identification of the anti-oral precancerous activity of GV

The chemical structure of GV was shown in Fig. 2A. We further tested the IC_{50} of GV in HOK normal epithelial cells, DOK oral precancerous cells and SAS oral cancer cells to verify the efficacy of GV. The IC_{50} for DOK cells was about 3.5 μM, while the IC_{50} for HOK and SAS cells were 5 μM and 9 μM respectively (Fig. 2B). Next, we determined GV-induced cell death and cell cycle distribution in oral precancerous cells. The sub-G1 population increased from 3% to 32% when the dose of GV was increased from 1 μM to 5 μM (Fig. 2C). To elucidate whether the sub-G1 cells were derived from apoptosis or necrosis, Annexin V staining was applied to confirm the cell death type. PI and Annexin V double positive cells significantly increased after DOK cells were treated with 3.5 μM GV for 24 h (Fig. 2D). Furthermore, we checked the expression of apoptosis-related proteins when DOK cells were treated with 3.5 μM GV for 2 h to 24 h. The expression level of the active forms of apoptotic markers including cleaved-PARP, cleaved-Caspase-3, cleaved-Caspase-9 and cleaved-Caspase-7 significantly increased in a time-dependent manner (Fig. 2E). Besides, the phosphorylation level of H2AX (γH2AX), a marker of apoptotic DNA fragmentation, was also markedly increased from 8 h to 24 h (Fig. 2E). Collectively, GV treatment led to apoptosis in oral precancerous cells.

3.3. ROS production was involved in GV-induced oral precancerous cell death

Next, we investigated the mechanisms underlying GV-induced apoptosis in oral precancerous cells. It is well known that reactive oxygen species (ROS) may induce DNA breaks and phosphorylation of H2AX [33]. We used two redox-sensitive fluorescent indicators, DCFDA and DHE, to determine the intracellular ROS levels. The fluorescent intensity of both $DCFDA^+$ cells and DHE^+ cells increased after DOK cells were treated with GV for 1 h (Fig. 3A). To verify whether ROS was involved in GV-induced cell death, we used the antioxidant, NAC, to study cell viability and cell cycle distribution. Cell viability was reduced to 50% after treatment with 3.5 μM GV, but increased to 70% when co-treated with NAC (Fig. 3B). Moreover, the sub-G1 population decreased from 20% to 5% when cells were co-treated with NAC (Fig. 3C).

3.4. Signaling pathways regulated by GV in oral precancerous cells

DNA damage may activate p53 through Ser15 phosphorylation, leading to cell cycle arrest, apoptosis or DNA repair [34]. Hence, we checked the level of p-p53 (S15) in GV-treated DOK cells and the result showed that the phosphorylation level of p-p53 (S15) was suppressed by GV from 0.5 h to 4 h (Fig. 4A). To test whether p53 is involved in GV-induced cell death, PFT-α was used to suppress p53 activity (Fig. 4B). In GV-treated DOK cells, the cell death was about 50% while co-treatment with p53 inhibitor increased the cell death proportion to 70% (Fig. 4B). While p53 activation is often related to apoptosis, its role in anti-apoptosis through the NFκB transcription factor has also been reported [35]. Indeed the phosphorylation level of NFκB in DOK cells was decreased when treated with 3.5 μM GV (Fig. 4A). Co-treatment with BAY11-7085, a NFκB inhibitor, and GV led to increased amount of cell death (Fig. 4C) and sub-G1 population (Fig. 4E).

3.5. GV inhibited the progression of oral precancerous lesions in vivo

In this study, hamsters were used as the *in vivo* model to explore the efficacy of GV on oral precancerous lesions. The orabase formulation for GV and the experimental design for hamster study have been described in the materials and methods section and the methodological flow chart is shown in Fig. 5A. The clinical appearance of buccal pouches showed no significant difference between untreated hamsters (Group A) and GV-treated hamsters (Group B). While there were no dyplastic changes on epithelium, the lamina propria became slightly thickened after GV treatment (Group B). However, visible tumors were observed in DMBA-treated hamsters (Group C), and decreased tumor volume was observed in DMBA-treated hamsters following 3% GV

treatment (Group D) (Fig. 5B). Moreover, the histology of buccal pouch lesions from Group C showed epithelial hyperplasia with moderate to severe epithelial dysplasia while the histology for buccal pouch lesions from Group D was similar to normal epithelium (Fig. 5B). After GV treatment for 3 weeks, the buccal pouch tumor volume in Group D was significantly smaller than Group C (Fig. 5C). Of note, no significant differences were observed in the blood biomedical parameters between Group C and Group D (Fig. 5D). Furthermore, the expression of p-p53(S15) and p-NFκB(S536) in group D was consistent with the *in vitro* results. We observed that the phosphorylation level of p53(S15) and NFκB(S536) was significantly lower in Group D than Group C (Fig. 5E). We also found that the expression of Ki67, the marker for proliferating cells, significantly decreased in Group D compared with Group C (Fig. 5E). Therefore, this new orabased formulation of GV effectively suppressed the progression of oral precancerous lesions.

4. Discussion

The purpose of this study is to develop orabased formulation for treatment of oral precancerous lesions through drug repurposing approach. In this study, we discovered by HTS analysis that gentian violet (GV), a clinically used drug for skin disinfection, induced apoptosis in DOK oral precancerous cells, and this was mediated by ROS production followed by suppression of p53 and NFκB signaling pathways. More importantly, we developed a new orabased formulation for GV which inhibited the progression of oral precancerous lesions in hamsters.

HTS has been a major approach to identify new biological and clinical drugs and a number of FDA-approved anti-cancer drugs have been discovered and developed by the HTS approach [36]. Its advantages include cost-effectiveness, parallel data generation, low-volume assay and speedy timeline for drug discovery [37]. Using the HTS approach, we discovered that GV could effectively suppress the progression of oral precancerous lesions.

The pro-apoptotic activity of p53 has been well documented, which is associated with its tumor suppressor functions. However, some studies have indicated that p53 is also an active transcription factor of pro-survival signaling pathways [35]. Inhibition of p53 expression has been shown to induce cell death and suppress tumor growth in ALT cancer cells through reduced AKT phosphorylation [38]. Indeed in the current study, we showed that GV-induced apoptosis was accompanied by decreased level of p-p53(Ser15), suggesting that the role of p53 in oral precancerous cells is oncogenic. More interestingly, in lung cancer cells and colon cancer cells, GV is dependent on p53 for inducing cell death [39]. Hence, the cell death signaling pathways mediated by GV may vary according to cancer type.

In the treatment of oral diseases, technological advances in mucoadhesives and sustained release could enhance therapeutic efficacy and reduce drug wastage by maintaining the drugs on oral mucosa and increasing patient compliance [40,41]. With these advantages, topical oral gels have been widely used as anti-inflammatory, anti-fungal and mucoprotective agents in the oral cavity [41]. In a previous study, 2% GV solution was used for oral hairy leukoplakia (OHL) derived from EBV infection [12]. Leukoplakia is defined as a type of OPMD and is associated with progression to OSCC [4]. Moreover, 2% GV in that study was formulated as a solution. In this study, we produced a new formulation of GV in orabase form. It has been known that OPMD is a local lesion in the oral cavity. Hence, orabase-formulated GV has greater potential opportunity for becoming a new therapeutic strategy for OPMD.

Drug repurposing is an effective strategy to identify new applications for previously approved clinical drugs [2]. Since most repurposed drugs have already passed the preclinical testing and safety assessment phases, drug repurposing has the potential to obtain approval in a more time-saving and cost-effective manner [42]. Based on all the provided evidence in this study, we propose that the orabase-formulated GV will have a faster track in terms of drug development for local non-invasive treatment of OPMD lesions after more extensive and stringent validation for its efficacy and side effect profile.

Using a HTS drug-repurposing approach followed by drug formulation and extensive *in vitro* and *in vivo* studies, we conclude that gentian violet (GV), a commercially available drug, may have a new biomedical indication in the treatment of oral precancerous lesions. Further preclinical and clinical studies are required to confirm its therapeutic potential for OPMD.

Acknowledgements

This study was supported by grant from the Ministry of Health and Welfare (MOHW108-TDU-B-212-124016, Health and welfare surcharge of tobacco products) of Taiwan, grant from Ministry of Education for Center For Intelligent Drug Systems and Smart Biodevices (IDS2B) from The Featured Areas Research Center Program within the framework of the Higher Education Sprout Project, grant from Kaohsiung Medical University (KMU-DK108005, KMU-Q108019, PT107003 and PT107004) , and Kaohsiung Medical University Research Center Grant (KMU-TC108A04). The authors would like to thank ChemBank HTS Resource Center (SB1) of National Research Program for Biopharmaceuticals (NRPB) for their service.

References

[1] C. Rivera, B. Venegas, Histological and molecular aspects of oral squamous cell carcinoma (Review), Oncol. Lett. 8 (1) (2014) 7–11.
[2] J.J. Sciubba, Oral cancer. The importance of early diagnosis and treatment, Am. J. Clin. Dermatol. 2 (4) (2001) 239–251.
[3] I. Gomez, J. Seoane, P. Varela-Centelles, P. Diz, B. Takkouche, Is diagnostic delay related to advanced-stage oral cancer? A meta-analysis, Eur. J. Oral Sci. 117 (5) (2009) 541–546.
[4] S.L. Chuang, C.P. Wang, M.K. Chen, W.W. Su, C.W. Su, S.L. Chen, et al., Malignant transformation to oral cancer by subtype of oral potentially malignant disorder: a prospective cohort study of Taiwanese nationwide oral cancer screening program, Oral Oncol. 87 (2018) 58–63.
[5] A.M. Yen, S.C. Chen, S.H. Chang, T.H. Chen, The effect of betel quid and cigarette on multistate progression of oral pre-malignancy, J. Oral Pathol. Med. 37 (7) (2008) 417–422.
[6] M.J. McCullough, G. Prasad, C.S. Farah, Oral mucosal malignancy and potentially malignant lesions: an update on the epidemiology, risk factors, diagnosis and management, Aust. Dent. J. 55 (Suppl 1) (2010) 61–65.
[7] H. Gelband, P. Jha, R. Sankaranarayanan, S. Horton, Cancer: Disease Control Priorities. Third ed. Vol. 3. 2015.
[8] A.M. Maley, J.L. Arbiser, Gentian violet: a 19th century drug re-emerges in the 21st century, Exp. Dermatol. 22 (12) (2013) 775–780.
[9] Meng Sun, K. Ricker, Gwendolyn Osborne, M. Elizabeth Marder, Rose Schmitz, Evidence on the Carcinogenicity of Gentian Violet. 2018. p1–117.
[10] B.N. Perry, B. Govindarajan, S.S. Bhandarkar, U.G. Knaus, M. Valo, C. Sturk, et al., Pharmacologic blockade of angiopoietin-2 is efficacious against model hemangiomas in mice, J, Invest. Dermatol. 126 (10) (2006) 2316–2322.
[11] J.L. Arbiser, M. Bips, A. Seidler, M.Y. Bonner, C. Kovach, Combination therapy of imiquimod and gentian violet for cutaneous melanoma metastases, J. Am. Acad. Dermatol. 67 (2) (2012) e81–e83.
[12] S.S. Bhandarkar, J. MacKelfresh, L. Fried, J.L. Arbiser, Targeted therapy of oral hairy leukoplakia with gentian violet, J. Am. Acad. Dermatol. 58 (4) (2008) 711–712.
[13] H.P. Varbanov, F. Kuttler, D. Banfi, G. Turcatti, P.J. Dyson, Repositioning approved drugs for the treatment of problematic cancers using a screening approach, PLoS ONE 12 (2) (2017) e0171052.
[14] Y.J. Chen, H.P. Chen, Y.J. Cheng, Y.H. Lin, K.W. Liu, Y.J. Chen, et al., The synthetic flavonoid WYC02-9 inhibits colorectal cancer cell growth through ROS-mediated activation of MAPK14 pathway, Life Sci. 92 (22) (2013) 1081–1092.
[15] L.H. Li, P. Wu, J.Y. Lee, P.R. Li, W.Y. Hsieh, C.C. Ho, et al., Hinokitiol induces DNA damage and autophagy followed by cell cycle arrest and senescence in gefitinib-resistant lung adenocarcinoma cells, PLoS ONE 9 (8) (2014) e104203.
[16] < 2001 Oral Cancer.pdf > .
[17] S. Smith, J. Fox, M. Mejia, W. Ruangpradit, A. Saberi, S. Kim, et al., Histone deacetylase inhibitors selectively target homology dependent DNA repair defective cells and elevate non-homologous endjoining activity, PLoS ONE 9 (1) (2014) e87203.
[18] S. Hong, P. Hu, E. Roessler, T. Hu, M. Muenke, Loss-of-function mutations in FGF8 can be independent risk factors for holoprosencephaly, Hum. Mol. Genet. 27 (11) (2018) 1989–1998.
[19] K.K. Liu, W.R. Qiu, E. Naveen Raj, H.F. Liu, H.S. Huang, Y.W. Lin, et al., Ubiquitin-coated nanodiamonds bind to autophagy receptors for entry into the selective autophagy pathway, Autophagy 13 (1) (2017) 187–200.
[20] U. Sahu, A. Choudhury, S. Parvez, S. Biswas, S. Kar, Induction of intestinal stemness

and tumorigenicity by aberrant internalization of commensal non-pathogenic E. coli, Cell Death Dis. 8 (3) (2017) e2667.
[21] C. Lv, H.W. Zeng, J.X. Wang, X. Yuan, C. Zhang, T. Fang, et al., The antitumor natural product tanshinone IIA inhibits protein kinase C and acts synergistically with 17-AAG, Cell Death Dis. 9 (2) (2018) 165.
[22] Y. Hotokezaka, I. Katayama, K. van Leyen, T. Nakamura, GSK-3beta-dependent downregulation of gamma-taxilin and alphaNAC merge to regulate ER stress responses, Cell Death Dis. 6 (2015) e1719.
[23] J.H. Feng, K. Nakagawa-Goto, K.H. Lee, L.F. Shyur, A novel plant sesquiterpene lactone derivative, DETD-35, suppresses BRAFV600E mutant melanoma growth and overcomes acquired vemurafenib resistance in mice, Mol. Cancer Ther. 15 (6) (2016) 1163–1176.
[24] P. Xu, X. Tao, C. Zhao, Q. Huang, H. Chang, N. Ban, et al., DTX3L is upregulated in glioma and is associated with glioma progression, Int. J. Mol. Med. 40 (2) (2017) 491–498.
[25] D. Zhang, L. Li, H. Jiang, B.L. Knolhoff, A.C. Lockhart, A. Wang-Gillam, et al., Constitutive IRAK4 activation underlies poor prognosis and chemoresistance in pancreatic ductal adenocarcinoma, Clin. Cancer Res. 23 (7) (2017) 1748–1759.
[26] I.B. Gimenez-Conti, T.J. Slaga, The hamster cheek pouch carcinogenesis model, J. Cell. Biochem. Suppl. 17f (1993) 83–90.
[27] G. Shklar, E. Eisenberg, E. Flynn, Immunoenhancing agents and experimental leukoplakia and carcinoma of the hamster buccal pouch, Prog. Exp. Tumor Res. 24 (1979) 269–282.
[28] Y.K. Chen, L.M. Lin, DMBA-induced hamster buccal pouch carcinoma and VX2-induced rabbit cancer as a model for human oral carcinogenesis, Expert Rev. Anticancer Ther. 10 (9) (2010) 1485–1496.
[29] M. Sarbia, M. Stahl, U. Fink, R. Willers, S. Seeber, H.E. Gabbert, Expression of apoptosis-regulating proteins and outcome of esophageal cancer patients treated by combined therapy modalities, Clin. Cancer Res. 4 (12) (1998) 2991–2997.
[30] M.N. Jabbour, G. Issa, K. Charafeddine, Y. Simaan, M. Karam, H. Khalifeh, et al., The immune microenvironment in cutaneous leishmaniasis, J. Eur. Acad. Dermatol. Venereol. 29 (6) (2015) 1170–1179.
[31] Z. Gao, X. Meng, D. Mu, X. Sun, J. Yu, Prognostic significance of epidermal growth factor receptor in locally advanced esophageal squamous cell carcinoma for patients receiving chemoradiotherapy, Oncol. Lett. 7 (4) (2014) 1118–1122.
[32] J.Y. Kim, G.H. Ko, Y.J. Lee, W.S. Ha, S.K. Choi, E.J. Jung, et al., Prognostic value of sonic hedgehog protein expression in gastric cancer, Jpn. J. Clin. Oncol. 42 (11) (2012) 1054–1059.
[33] Z. Li, J. Yang, H. Huang, Oxidative stress induces H2AX phosphorylation in human spermatozoa, FEBS Lett. 580 (26) (2006) 6161–6168.
[34] N.D. Lakin, S.P. Jackson, Regulation of p53 in response to DNA damage, Oncogene 18 (53) (1999) 7644–7655.
[35] R.U. Janicke, D. Sohn, K. Schulze-Osthoff, The dark side of a tumor suppressor: anti-apoptotic p53, Cell Death Differ. 15 (6) (2008) 959–976.
[36] N.P. Coussens, J.C. Braisted, T. Peryea, G.S. Sittampalam, A. Simeonov, M.D. Hall, Small-molecule screens: a gateway to cancer therapeutic agents with case studies of food and drug administration-approved drugs, Pharmacol. Rev. 69 (4) (2017) 479–496.
[37] R. Macarron, M.N. Banks, D. Bojanic, D.J. Burns, D.A. Cirovic, T. Garyantes, et al., Impact of high-throughput screening in biomedical research, Nat. Rev. Drug Discov. 10 (3) (2011) 188–195.
[38] Y. Ge, S. Wu, Z. Zhang, X. Li, F. Li, S. Yan, et al., Inhibition of p53 and/or AKT as a new therapeutic approach specifically targeting ALT cancers, Protein Cell (2019) 1–17.
[39] A. Garufi, V. D'Orazi, J.L. Arbiser, G. D'Orazi, Gentian violet induces wtp53 transactivation in cancer cells, Int. J. Oncol. 44 (4) (2014) 1084–1090.
[40] V. Hearnden, V. Sankar, K. Hull, D.V. Juras, M. Greenberg, A.R. Kerr, et al., New developments and opportunities in oral mucosal drug delivery for local and systemic disease, Adv. Drug Deliv. Rev. 64 (1) (2012) 16–28.
[41] A. Priprem, C. Nukulkit, N.P. Johns, T. Damrongrungruang, N. Wongsangta, E.O. Benjavongkulchai, Effect of polymeric combinations on mucoadhesive and swelling properties of orabase gel formulations, Adv. Mater. Res. 853 (2013) 3–8.
[42] S. Pushpakom, F. Iorio, P.A. Eyers, K.J. Escott, S. Hopper, A. Wells, et al., Drug repurposing: progress, challenges and recommendations, Nat. Rev. Drug Discov. 18 (1) (2019) 41–58.